Journal of Circuits, Systems, and Computers, Vol. 9, Nos. 3 & 4 (1999) 229–242

CHAOTIC OSCILLATOR CONFIGURATION USING A FREQUENCY DEPENDENT NEGATIVE RESISTOR

A. S. ELWAKIL and M. P. KENNEDY
Department of Electronic & Electrical Engineering,
University College Dublin, Dublin 4, Ireland

Received 2 October 1998
Accepted 17 June 1999

Chaos is observed from a fourth-order autonomous circuit inspired by Chua's circuit and obtained by replacing the active symmetric nonlinear resistor (Chua's diode) with a parallel combination of a frequency dependent negative resistor (FDNR) and a general-purpose signal diode. Accordingly, nonlinearity is introduced by a passive device with antisymmetric current-voltage characteristics whereas activity is transferred to the FDNR. The observed chaotic attractor has similar dynamics to the *Colpitts* chaotic attractor and we show its topological equivalence to the well-known *Rossler* attractor. Experimental results, PSpice simulations and numerical simulations of the derived mathematical models are included.

1. Introduction

Since its discovery, Chua's circuit has served as the main prototype circuit for studying chaos in electronic systems.[1] Several realizations of this circuit have thus been introduced in the literature.[2–7] It can be identified from Refs. 2–7 that the most difficult part to realize in Chua's circuit is the active nonlinear resistor (Chua's diode) which is approximated by a three-segment piecewise linear I–V characteristic. In fact, on the route to producing a monolithic implementation of the circuit, a nonlinear resistor was separately designed[3] prior to integrating the whole circuit.[4] The approach used in Refs. 3–7 was based upon the standard implementation of Ref. 2 in which two op amps, one of which behaves linearly while the other behaves nonlinearly, in addition to six resistors, are required to implement Chua's diode. The functionality of the op amps can be reproduced using other building blocks such as operational transconductance amplifiers (OTAs)[5] or current feedback op amps (CFOAs).[6,7] It has also been shown that a cubic nonlinearity can produce qualitatively similar dynamics.[8] However, the realization of such a nonlinearity requires several analog multipliers, which are complicated to design.

Recently, several new designs for chaotic oscillators have been reported[9–14] motivated by the observation of chaos in the classical Colpitts oscillator.[15] A common feature of all the oscillators in Refs. 9–14 is the use of simple passive nonlinear devices such as diodes or diode-connected transistors. The design rules proposed in Refs. 16 and 17 recommend the use of passive nonlinear devices since there is no evidence that the chaotic signal produced by a system with active nonlinearity

possesses any statistical feature not possessed by a system with a passive nonlinearity. Furthermore, chaotic oscillators with a passive nonlinearity can be optimized using classical optimization techniques for linear systems and their performance can be evaluated according to linear design benchmarks.

In this work, a new chaotic oscillator configuration, inspired by Chua's circuit, is proposed. The passive structure in Chua's circuit is preserved while the active nonlinear resistor is replaced by a parallel combination of a frequency dependent negative resistor (FDNR) and a switching diode. The observed chaotic attractor is governed by similar dynamics to the chaotic Colpitts attractor,[18,19] as expected. We investigate briefly the relationship between the well-known Rossler system and Colpitts-like chaotic oscillators. In particular, we show that the dynamics of Rossler's system in the X–Y plane are those of a simple sinusoidal oscillator, similar to all Colpitts-like oscillators. We then propose a modified Rossler system with a switching-type nonlinearity, instead of the multiplier-type nonlinearity, and demonstrate its topological equivalence to Colpitts-like chaotic oscillators.

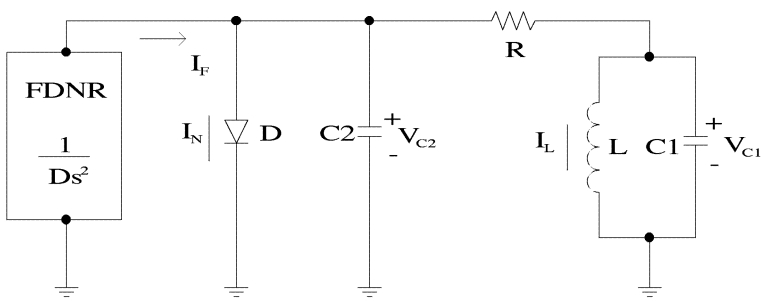

Fig. 1. Modified Chua's circuit using a parallel FDNR-diode combination to replace the active nonlinear resistor.

2. The New FDNR-Based Chaotic Oscillator

Figure 1 shows our new chaotic oscillator configuration obtained by replacing the active odd-symmetric nonlinear resistor in Chua's circuit with an FDNR and a signal diode. The FDNR is a well-known linear analog building block that was derived from general impedance converters (GICs) and introduced to realize inductorless active filters by applying Bruton's transformation.[20] The input impedance of an FDNR circuit is equal to $1/Ds^2$, where D has the units of Farad. Sec and s is the complex radian frequency ($j\omega$). Considering a practical realization of an FDNR, the parameter D can be written in the form $D = C_F^2 R_F / K$, where K is a scaling factor, C_F and R_F are the equivalent capacitance and resistance used to realize the FDNR. This is also demonstrated in the next section where an FDNR derived from Antoniou's GIC[21] is constructed.

Denoting the FDNR current by I_F, the nonlinear diode current by I_N and using a two-segment piecewise linear approximation of the diode current-voltage

characteristic, the configuration in Fig. 1 can be described by the following set of differential equations:

$$\begin{aligned} C_1\dot{V}_{C1} &= \frac{V_{C2}-V_{C1}}{R} - I_L \\ C_2\dot{V}_{C2} &= I_F - I_N - \frac{V_{C2}-V_{C1}}{R} \\ L\dot{I}_L &= V_{C1}\,, \end{aligned} \tag{1a}$$

where

$$I_F = -D\ddot{V}_{C2} \qquad \text{and} \qquad I_N = \frac{1}{R_D}\begin{cases} V_{C2}-V_\gamma & V_{C2} \geq V_\gamma \\ 0 & V_{C2} < V_\gamma \end{cases} \tag{1b}$$

R_D and V_γ are the diode forward conduction resistance and voltage drop respectively.

Because of the diode's antisymmetrical characteristic, the chaotic attractor observed from this oscillator is expected to resemble that of the chaotic Colpitts oscillator.[15,18] Recalling that $D = C_F^2 R_F/K$ and by introducing the following dimensionless quantities:

$$\tau = \frac{t}{C_F R}, \quad X = \frac{V_{C1}}{V_\gamma}, \quad Y = \frac{V_{C2}}{V_\gamma}, \quad Z = \frac{RI_L}{V_\gamma}, \quad \alpha = \frac{R}{R_D}, \quad \beta = \frac{C_F R^2}{L},$$
$$\varepsilon_1 = \frac{C_1}{C_F}, \quad \varepsilon_2 = \frac{C_2}{C_F}, \quad K_1 = \frac{R}{R_F},$$

equation set (1) transforms into:

$$\begin{aligned} \varepsilon_1\dot{X} &= Y - X - Z \\ \frac{K_1}{K}\ddot{Y} &= X - Y - \varepsilon_2\dot{Y} - f(Y) \\ \dot{Z} &= \beta X \end{aligned} \tag{2a}$$

and

$$f(Y) = \alpha\begin{cases} Y-1 & Y \geq 1 \\ 0 & Y < 1 \end{cases}. \tag{2b}$$

Numerical integration of (2) was carried out using a Runge-Kutta fourth-order algorithm with a 0.001 time step taking $\varepsilon_1 = \beta = 0.01$, $\varepsilon_2 = 1$, $\alpha = 50$, and $K_1/K = 12.5$. A projection in the Y–Z plane of the observed chaotic attractor is plotted in Fig. 2. This attractor is preserved when integrating (2) with either ε_1 or ε_2 as small as 0.0001, which indicates that although the system described by (2) is fourth-order, the attractor is effectively living in a three dimensional subspace. However, care should be taken in numerical integrations with such small values of ε_1 and ε_2.

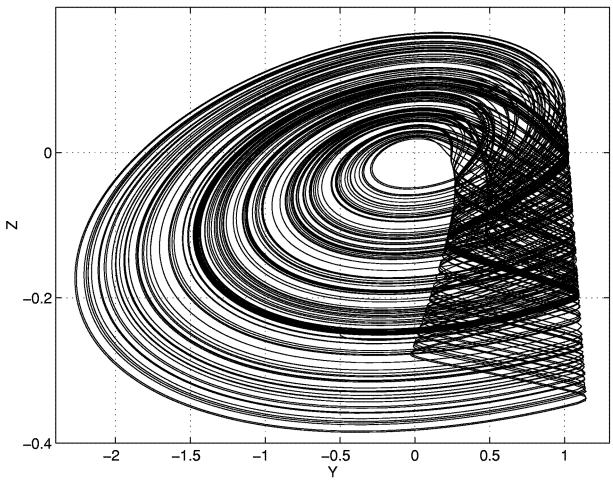

Fig. 2. Y–Z phase space trajectory obtained by numerically integrating (2).

From a practical point of view, the values of ε_1 and ε_2 should be chosen to facilitate any possible circuit implementation. The three design sets: ($\varepsilon_1 = \varepsilon_2 = 1$), ($\varepsilon_1 = 1, \varepsilon_2 = \Delta$) and ($\varepsilon_1 = \Delta, \varepsilon_2 = 1$), where Δ is practically small, are particularly useful. The first set allows all capacitors used in the circuit to have equal values, which might be desirable in some implementations. The other two sets allow one of the capacitors C_1 or C_2 to be a parasitic capacitor.

Note also that the ratio between K and K_1, rather than their absolute values, is significant. Thus, the circuit dynamics can be varied either through the floating resistor R, as with Chua's circuit, or through the FDNR scaling factor K which provides tunability via a single grounded resistor, as shown in the implementation presented in Sec. 3. Using either of these two parameters as the bifurcation parameter, a period-doubling route to chaos is observed.

A state space representation of (2) can be obtained by introducing a new state variable W, equal to $\dot{Y}$, which results in the following matrix form:

$$\begin{bmatrix} \varepsilon_1 \dot{X} \\ \dot{Y} \\ \dot{Z} \\ \dfrac{K_1}{K} \dot{W} \end{bmatrix} = \begin{bmatrix} -1 & 1 & -1 & 0 \\ 0 & 0 & 0 & 1 \\ \beta & 0 & 0 & 0 \\ 1 & -(1+a) & 0 & -\varepsilon_2 \end{bmatrix} \begin{bmatrix} X \\ Y \\ Z \\ W \end{bmatrix} + \begin{bmatrix} 0 \\ 0 \\ 0 \\ a \end{bmatrix}, \tag{3a}$$

where

$$a = \begin{cases} \alpha & Y \geq 1 \\ 0 & Y < 1 \end{cases}. \tag{3b}$$

The system described by (3a) has an equilibrium point in each of the two regions of operation of (3b). These equilibrium points are given by: $(x_0, y_0, z_0, w_0) =$

$\frac{a}{1+a}(0,1,1,0)$. Thus, there is a single equilibrium point at the origin in the region $Y < 1$. The equilibrium point in the region $Y \geq 1$ is virtual, meaning that it lies outside this region.[22] For the parameter values used in numerical simulation, the equilibrium point in the region $Y < 1$ has the set of eigenvalues: $(-0.1312, -99.99, 0.0202 \pm j0.0754)$ which indicates that it is an unstable focus. The set of eigenvalues: $(-0.0102, -99.99, -0.0403 \pm j1.9996)$ corresponds to the virtual equilibrium point in the region $Y \geq 1$, indicating that it is stable. Therefore, assuming that the circuit starts with the diode initially off ($Y < 1$), the V_{C1}, V_{C2} and I_L trajectories will be repelled by the unstable equilibrium point at the origin and will spiral outwards due to the complex conjugate pair of eigenvalues. Eventually, this will cause the diode to turn on when V_{C2} exceeds $V_\gamma (Y \geq 1)$. Since the equilibrium point in this region is stable, the trajectories will be attracted towards it. However, before reaching this stable equilibrium point, which lies in the region $Y < 1$, the diode switches off again and the spiral out motion of the trajectories repeats. These qualitative dynamics are typical for Colpitts-like chaotic oscillators[9–15] and have been studied in detail for the Colpitts oscillator in Refs. 19.

3. PSpice Simulations and Experimental Results

In order to verify experimentally the performance of the proposed circuit, a classical FDNR implementation based on Antoniou's GIC[21] is constructed. As shown in Fig. 3(a), this realization requires two op amps (both operating in their linear regions), two equal capacitors denoted by C_F, and three resistors (R_1, R_2, R_3). Routine analysis shows that $D = C_F^2 R_1 R_2 / R_3$. Hence, the choice of $R_1 = R_2 = R_F$ and $R_3 = KR_F$ results in $D = C_F^2 R_F / K$. PSpice simulations of the chaotic oscillator in Fig. 3(a) were carried out with $C_1 = 100$ pF, $C_2 = C_F = 1$ nF, $L = 47$ mH, $R_1 = R_2 = 3$ kΩ, $R_3 = 1.2$ kΩ and $R = 150$ Ω. A general purpose diode of type D1N914 was used and the op amps were biased with ±9 V supplies. The observed $V_{C2} - I_L$ projection of the resulting attractor is shown in Fig. 3(b), corresponding to the Y–Z trajectory of Fig. 2. Here we have used a small value for C_1 to demonstrate that it can become a parasitic.

The circuit can be tuned through a period-doubling cascade by varying K using the grounded resistor R_3. It is worth noting that since the circuit model does not depend on any circuit-specific parameter of the FDNR, any suitable realization of an FDNR might be used. It is thus possible to optimize this FDNR to satisfy constraints imposed on the circuit's power dissipation, frequency response or supply voltage. From an analog design point of view, it is easier to optimize an FDNR than an active nonlinear resistor such as Chua's diode.

An experimental setup of the circuit was constructed with the same component values used in the PSpice simulations taking, R equal to 500 Ω and R_3 as a 5 kΩ pot. for tuning. A current-to-voltage converter with a 1 kΩ load was used to convert the coil current to a voltage V_L. The resulting $V_{C2} - V_L$ phase portrait is shown in Fig. 4. The qualitative agreement with numerical and PSpice simulations is clear.

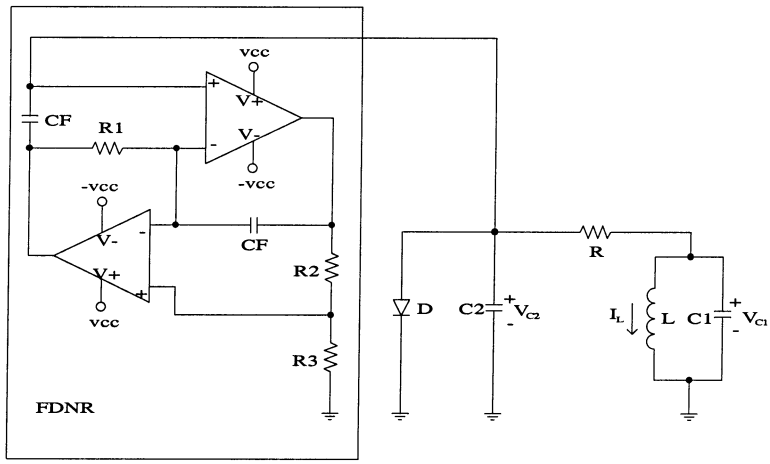

(a)

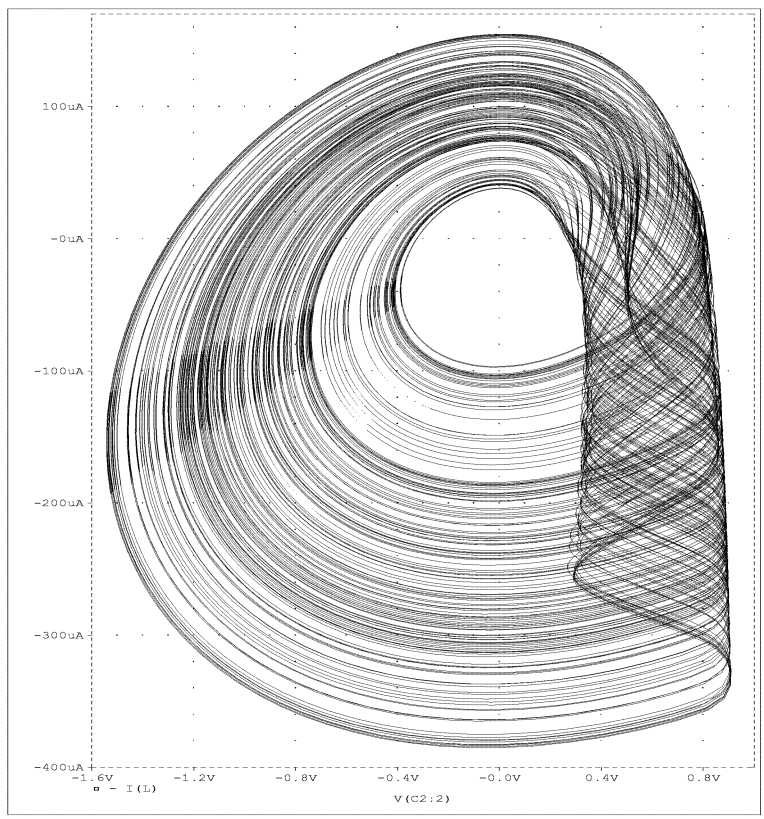

(b)

Fig. 3. (a) Implementation of the modified Chua's circuit using Antoniou's GIC. (b) PSpice simulation of the $V_{C2} - I_L$ trajectory.

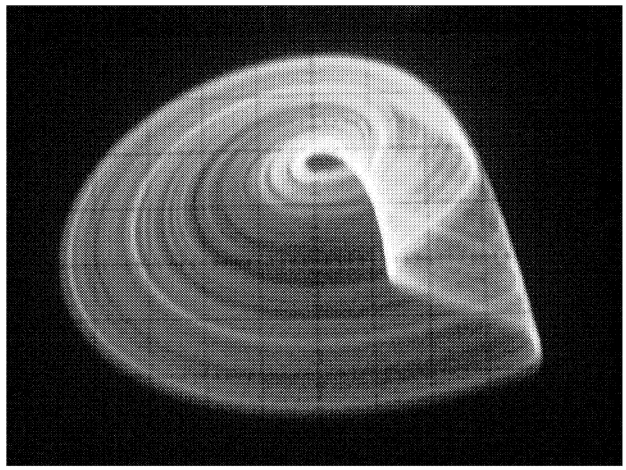

Fig. 4. Experimentally observed $V_{C2} - V_L$ trajectory. X axis: 0.1 V/div. Y axis: 0.1 V/div.

4. Connection between Rossler's System and Colpitts-like Chaotic Oscillators

The similarity between the chaotic attractor observed from our new FDNR-based chaotic oscillator and the well-known Rossler attractor has been brought to our notice by a reviewer. In fact, this similarity holds for all Colpitts-like chaotic attractors. However, the nature of the nonlinearity in Rossler's system is significantly different from that in any of the Colpitts-like oscillators.[9–15] In particular, the nonlinearity in Rossler's system is obtained by multiplying two state variables, whereas the nonlinearity in Colpitts-like chaotic oscillators is obtained by switching a constant parameter between two values when one (or more) of the state variables hits a threshold value. This switching-type nonlinearity typically reflects the behavior of a simple diode. Furthermore, all Colpitts-like chaotic oscillators have a core sinusoidal oscillator engine which is responsible for stretching the trajectories.

In order to establish the connection between Rossler's system and Colpitts-like chaotic oscillators, two steps are required. The first is to show that Rossler's system has a core sinusoidal oscillator engine in the X–Y plane and that its chaotic behavior is preserved when different engines are used. The second step is to replace the multiplier-type nonlinearity in Rossler's system by a switching-type nonlinearity and to confirm the chaotic behavior of the resulting system (which is even more similar to Colpitts-like attractors). We then show that this modified Rossler system has a single unstable equilibrium point at the origin in one of the two regions of operation of the nonlinearity and an equilibrium point which is virtual and stable in the other region. Thus, it is governed by dynamics similar to those of the Colpitts oscillator, studied in Ref. 19.

4.1. *Dynamics in the X–Y plane*

Consider the classical Rossler's system[23] which is described by:

$$\dot{X} = -Y - Z \tag{4a}$$

$$\dot{Y} = X + AY \tag{4b}$$

$$\dot{Z} = -CZ + (B + Z)X\,, \tag{4c}$$

where A, B, and C are constants. The nonlinear term appears in (4c) as XZ.

It can be shown that the dynamics of (4) in the X–Y plane are given by:

$$\begin{bmatrix} \dot{X} \\ \dot{Y} \end{bmatrix} = \begin{bmatrix} 0 & -1 \\ 1 & A \end{bmatrix} \begin{bmatrix} X \\ Y \end{bmatrix} = [A] \begin{bmatrix} X \\ Y \end{bmatrix}. \tag{5}$$

We recall that a general second-order sinusoidal oscillator is described by:

$$\begin{bmatrix} \dot{X} \\ \dot{Y} \end{bmatrix} = \begin{bmatrix} a_{11} & a_{12} \\ a_{21} & a_{22} \end{bmatrix} \begin{bmatrix} X \\ Y \end{bmatrix} \tag{6a}$$

with a condition for oscillation and a frequency of oscillation given respectively by:

$$a_{11} + a_{22} = 0 \qquad \text{and} \qquad \omega_0 = \sqrt{a_{11}a_{22} - a_{12}a_{21}}\,. \tag{6b}$$

In the special case where $a_{11} = a_{22} = 0$, the sinusoidal oscillator is known as the two-integrator-loop quadrature oscillator. By comparing (5) and (6), it should be clear that the condition $A = 0$ implies that the dynamics of the Rossler system in the X–Y plane are those of the quadrature oscillator. The constant A is usually denoted by ε (error factor) since in practice it needs to be increased slightly above zero to start oscillations, i.e. to push the pair of complex conjugate eigenvalues slightly into the right half plane. Of course, an amplitude control mechanism (which is usually a saturation-type nonlinearity such as that of an op amp) is required to stabilize the amplitude of oscillation.

In order to show that the chaotic system of (4) requires a generic sinusoidal oscillator in the X–Y plane we consider the following four matrices which are dynamically equivalent:

$$\begin{bmatrix} 0 & -1 \\ 1 & A \end{bmatrix} \approx \begin{bmatrix} 0 & 1 \\ -1 & A \end{bmatrix} \approx \begin{bmatrix} A & 1 \\ -1 & 0 \end{bmatrix} \approx \begin{bmatrix} A & -1 \\ 1 & 0 \end{bmatrix}. \tag{7}$$

The system of (4) was integrated using the conventional parameter set $(A, B, C) = (0.36, 0.4, 5.7)$ with the X–Y plane dynamics governed by each of the above matrices. The Rossler attractor or its mirror-image was observed in each case. We note that since the X and Y state variables together represent a single entity (a quadrature oscillator), the term $-Z$ which appears in (4a) can appear in (4b) instead. Thus, both $\dot{X}$ and $\dot{Y}$ can be used to sense the changes along the Z direction. In general,

the strength of this sensing can be either enhanced or suppressed by a constant multiplication factor m. Hence, the term $-Z$ should more generally read $-mZ$.

4.2. *Nonlinear subsystem*

Equation (4c) can be considered as a separate nonlinear subsystem which is linked to the dynamics in the X–Y plane through the state variable X. The way this nonlinear subsystem works is very similar to a threshold-based nonlinear device. When the amplitude of the X signal is sufficiently small, the term $-CZ$ dominates the nonlinear term $(B+Z)X$. Hence, by neglecting the effect of this nonlinear term it can be shown that Z scales as e^{-Ct} which indicates that the amplitude of the Z signal rapidly decays with time. This allows the dynamics in the X–Y plane to be dominated by the sinusoidal oscillator (the term $-Z$ in (4a) is small and can be neglected) and thus oscillations rapidly build up. However, as the amplitude of X continues to increase, the nonlinear term can no longer be neglected and is eventually activated (switches on) resulting in a 'bursting' increase in the amplitude of Z. This in turn reflects back to Eq. (4a) causing the amplitudes of X and Y to decrease rapidly. Accordingly, the nonlinear term is then deactivated (switched off) and the oscillation in the X–Y plane starts building-up again.

The "bursting" increase in the amplitude of Z when the nonlinear term is activated actually indicates that most of the energy stored in the sinusoidal oscillator is suddenly transferred to (dissipated by) the nonlinear subsystem. This highlights the role of the constant B which controls this energy transfer. Too small a value for B results in more accumulation of energy on the oscillator side and thus the trajectories diverge and become unbounded (active devices saturate). Too large a value for B results in heavy dissipation of the generated energy and eventually the oscillations die.

Due to this understanding of the qualitative behavior of Rossler's system, we suggest that the nonlinear term $(B+Z)X$ can be replaced by other nonlinear terms which are independent of Z. Indeed, we have confirmed the observation of chaos with the nonlinear term $(B+X)Y$, as shown in Fig. 5(a), which represents the X–Y trajectory obtained by integrating (4) with $A = 0.36$, $B = 0.4$ and $C = 1.5$. Similar results can be obtained with the nonlinear term $(B+Y)X$.

4.3. *Modified rossler system*

We propose a modified Rossler system with a switching-type nonlinearity instead of the multiplier-type nonlinearity. Thus, the nonlinear subsystem described by (4c) is modified to be:

$$\dot{Z} = -CZ + BX\,, \tag{8a}$$

where either B or C is a switching term given by:

$$(B \text{ or } C) = \begin{cases} \alpha_1 & f(X,Y) \geq 1 \\ \alpha_2 & f(X,Y) < 1 \end{cases}. \tag{8b}$$

(a)

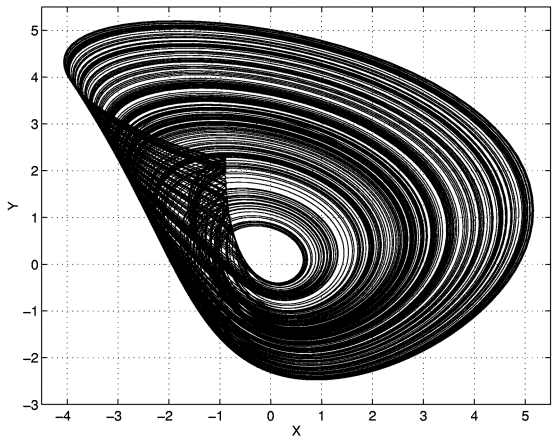

(b)

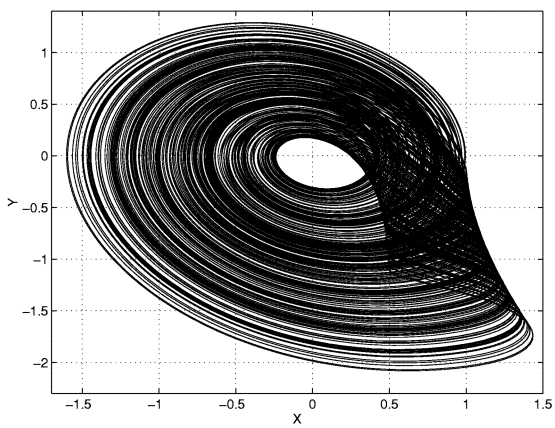

(c)

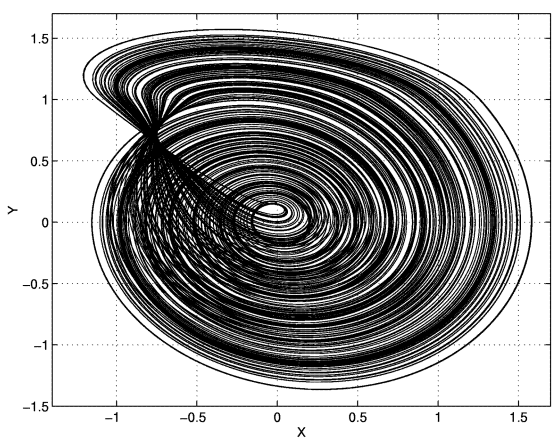

Fig. 5. (a) X–Y trajectory when Rossler's system of (4) is integrated with the nonlinear term $(B + X)Y$. $A = 0.36$, $B = 0.4$ and $C = 1.5$; (b) X–Y trajectory obtained after modifying (4) with (8) when $f(X, Y) = X$. $A = 0.3$, $C = 1.2$, $\alpha_1 = 4$ and $\alpha_2 = 0$; and (c) X–Y trajectory obtained after modifying (4) with (8) when $f(X, Y) = Y$. $A = 0.2$, $C = 0.8$, $\alpha_1 = 4$ and $\alpha_2 = 0$.

Two cases for $f(X,Y)$ are investigated, namely $f(X,Y) = X$ and $f(X,Y) = Y$. Figure 5(b) shows the X–Y trajectory observed when $A = 0.3$, $C = 1.2$ and B as given by (8b) with $f(X,Y) = X$, $\alpha_1 = 4$ and $\alpha_2 = 0$. The trajectory observed when $f(X,Y) = Y$ is shown in Fig. 5(c) with $A = 0.2$, $C = 0.8$ and the same B. A trajectory similar to that of Fig. 5(b) can also be observed with $A = 0.7$, $B = 1$ and C as given by (8b) with $f(X,Y) = X$, $\alpha_1 = 0$ and $\alpha_2 = 2$. Again, we stress that chaotic behavior persists when the dynamics in the X–Y plane are governed by any of the matrices in (7).

Our modified Rossler system can be written as:

$$\begin{bmatrix} \dot{X} \\ \dot{Y} \\ \dot{Z} \end{bmatrix} = \begin{bmatrix} 0 & -1 & -1 \\ 1 & A & 0 \\ B & 0 & -C \end{bmatrix} \begin{bmatrix} X \\ Y \\ Z \end{bmatrix}, \tag{9}$$

where either B or C are as given by (8b).

It can be seen that this system has a single equilibrium point at the origin in the region $f(X,Y) < 1$. The equilibrium point in the region $f(X,Y) \geq 1$ is virtual.[22] For the parameter values corresponding to Fig. 5(b), the equilibrium point at the origin has the set of eigenvalues: $(-1.2, 0.15 \pm j0.9887)$, which indicates that it is unstable, while the virtual equilibrium point has the set of eigenvalues $(0, -0.45 \pm j2.1065)$, which indicates that it is stable. For the parameter values corresponding to Fig. 5(c), the two sets of eigenvalues are: $(-0.8, 0.1 \pm j0.995)$ and $(0, -0.3 \pm j2.1794)$ respectively. These qualitative dynamics are typical for third-order Colpitts-like chaotic oscillators.[9–19]

Finally, we note that (9) can be written in the form:

$$\dddot{X} = -[(C - A)\ddot{X} + (1 + B - AC)\dot{X} + (C - AB)X] \tag{10}$$

where B or C are as given by (8b) with $f(X,Y) = f(\dot{X}, X)$.

For the choice of $C - A = 1$ and for sufficiently small values of A such that $A^2 \ll 1$, (10) simplifies to the following two-parameter system:

$$\dddot{X} = -[\ddot{X} + (1 - A + B)\dot{X} + (1 + A - AB)X]\,. \tag{11}$$

This system captures the dynamics of the modified Rossler system as seen in Figs. 6(a) and 6(b) which represent the $X - \dot{X}$ trajectory in the two cases $f(X, \dot{X}) = \dot{X}$ and $f(X, \dot{X}) = X$ respectively. Figure 6(a) was obtained with $A = 0.5$, $\alpha_1 = 5$ and $\alpha_2 = 0$ while Fig. 6(b) was obtained with A decreased to 0.2.

It is interesting to note that even the following single-parameter system captures the dynamics of Eq. (10):

$$\dddot{X} = -[\ddot{X} + B\dot{X} + X]\,, \tag{12}$$

where B is as given by (8b). Here α_1 is used as the bifurcation parameter. For the sack of clarity, we show the $X - \dot{X}$ trajectory in Fig. 6(c) with $\alpha_1 = 5$ and $\alpha_2 = 0$.

(a)

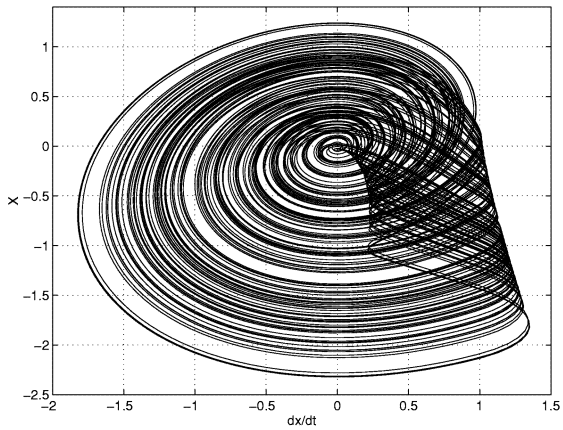

(b)

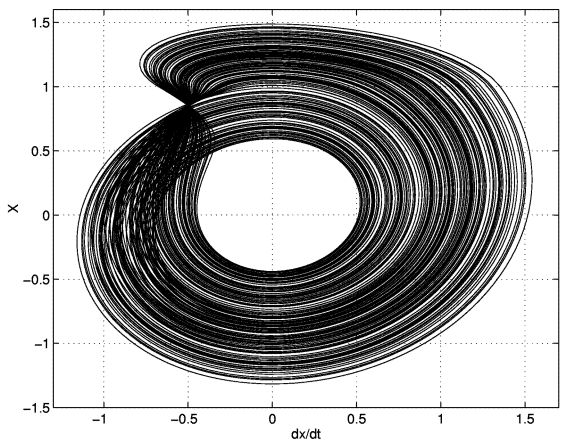

(c)

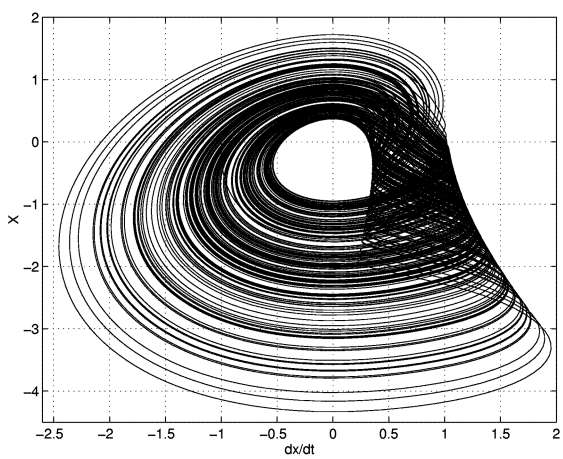

Fig. 6. (a); (b) $X - \dot{X}$ trajectory obtained by integrating (11) with $\alpha_1 = 5$ and $\alpha_2 = 0$ in the two cases $f(X, \dot{X}) = \dot{X}$ and $f(X, \dot{X}) = X$ respectively. $A = 0.5$ for (a) and $A = 0.2$ for (b); and (c) $X - \dot{X}$ trajectory obtained by integrating (12) with $\alpha_1 = 5$ and $\alpha_2 = 0$.

We suggest that Eqs. (11) and (12) capture in a canonical manner the qualitative dynamics of a large class of chaotic oscillators.

5. Conclusion

A new chaotic oscillator configuration using an FDNR-Diode combination has been reported. The chaotic attractor observed from this circuit is similar to the Colpitts attractor and is governed by similar dynamics. We have also established the connection between Rossler's system and Colpitts-like chaotic oscillators and have proposed a canonical version of this system using a switching-type nonlinearity.

Acknowledgment

The authors thank the reviewers for their useful comments. The AD713 op amps used in our experiments were provided by Analog Devices. This work was sponsored by the Enterprise Ireland Basic Research Programme under grant number SC/98/740.

References

1. G. Zhong and F. Ayrom, "Periodicity and chaos in Chua's circuit", *IEEE Trans. Circuits Syst.-I* **32** (1985) 501–505.
2. M. P. Kennedy, "Robust op amp realization of Chua's circuit", *Frequenz* **46** (1992) 66–80.
3. J. M. Cruz and L. O. Chua, "A CMOS IC nonlinear resistor for Chua's circuit", *IEEE Trans. Circuits Syst.-I* **39** (1992) 985–995.
4. J. M. Cruz and L. O. Chua, "An IC chip of Chua's circuit", *IEEE Trans. Circuits Syst.-II* **40** (1993) 614–625.
5. A. Rodriguez-Vazquez and M. Delgado-Restituto, "CMOS design of chaotic oscillators using state variables: a monolithic Chua's circuit", *IEEE Trans. Circuits Syst.-II* **40** (1993) 596–613.
6. R. Senani and S. S. Gupta, "Implementation of Chua's chaotic circuit using current feedback op amps", *Electron. Lett.* **34** (1998) 829–830.
7. A. S. Elwakil and M. P. Kennedy, "Improved implementation of Chua's chaotic oscillator using the current feedback op amp", *IEEE Trans. Circuits Syst.-I* (to appear).
8. G. Zhong, "Implementation of Chua's circuit with a cubic nonlinearity", *IEEE Trans. Circuits Syst.-I* **41** (1994) 934–941.
9. A. Namajunas and A. Tamasevicius, "Modified Wien-bridge oscillator for chaos", *Electron. Lett.* **31** (1995) 335–336.
10. A. S. Elwakil and A. M. Soliman, "Current mode chaos generator", *Electron. Lett.* **33** (1997) 1661–1662.
11. A. S. Elwakil and A. M. Soliman, "A family of Wien-type oscillators modified for chaos", *Int. J. Circuit Theor. Appl.* **25** (1997) 561–579.
12. A. S. Elwakil and A. M. Soliman, "Two Twin-T based op amp oscillators modified for chaos", *J. Franklin Inst.* **B335** (1998) 771–787.
13. A. S. Elwakil and M. P. Kennedy, "High frequency Wien-type chaotic oscillator", *Electron. Lett.* **34** (1998) 1161–1162.
14. A. S. Elwakil and M. P. Kennedy, "A family of Colpitts-like chaotic oscillators", *J. Franklin Inst.* **336** (1999) 687–700.

15. M. P. Kennedy, "Chaos in the Colpitts oscillator", *IEEE Trans. Circuits Syst.-I* **41** (1994) 771–774.
16. A. S. Elwakil and M. P. Kennedy, "Towards a methodology for designing autonomous chaotic oscillators", *Proc. 6th Int. Specialist Workshop Nonlinear Dynamics Elect. Syst.*
NDES'98, Budapest (1998).
17. A. S. Elwakil and M. P. Kennedy, "A semi-systematic procedure for producing chaos from sinusoidal oscillators using diode-inductor and FET-capacitor composites", *IEEE Trans. Circuits Syst.-I* (to appear).
18. M. P. Kennedy, "On the relationship between the chaotic Colpitts oscillator and Chua's oscillator", *IEEE Trans. Circuits Syst.-I* **42** (1995) 376–379.
19. G. M. Maggio, O. De Feo, and M. P. Kennedy, "Nonlinear analysis of the Colpitts oscillator and applications to design", *IEEE Trans. Circuits Syst.-I* **46** (1999) 1118–1129.
20. L. T. Bruton, "Network transfer functions using the concept of frequency-dependant negative-resistance", *IEEE Trans. Circuits Syst.-I* **16** (1969) 406–408.
21. A. Antoniou, "Realization of gyrators using operational amplifier", *Electron. Lett.* **3** (1967) 350–352.
22. L. O. Chua, C. A. Desoer, and E. S. Kuh, *Linear and Nonlinear Circuits*, McGraw-Hill, 1987.
23. O. E. Rossler, "An equation for continuous chaos", *Phys. Lett.* **A57** (1976) 397–398.